Neutral pion polarizabilities from four-point functions

Frank Lee (GW)
Collaborators: Walter Wilcox (Baylor), Andrei Alexandru (GW), Chris Culver (Liverpool), Shayan Nadeem (Baylor)

Outline

1) Motivation
2) Background field vs four-point function
3) Lattice simulation and results
4) Conclusion

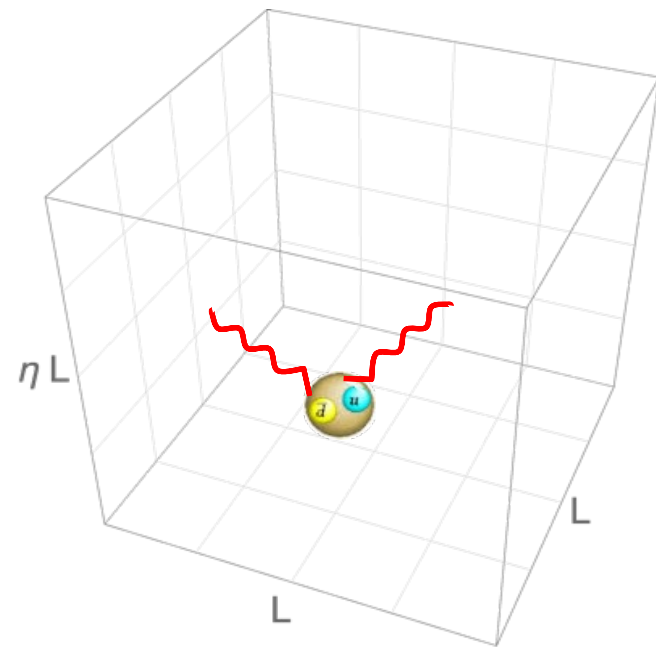

Supported in part by U.S. Department of Energy grant DE-FG02-95ER40907

Lattice 2024, August 1, Liverpool

Hadron polarizabilities (in units of 10^{-4} fm^3)

- Polarizabilities encode information on charge and current distributions inside hadrons at low energies.
- An active community in nuclear physics is engaged in the effort (experiment, theory, lattice QCD)

1) Hadrons are stiff compared to H-atom ($\alpha=4.5\ a_0^3$)
2) QCD+QED

Charged pion ($\pi^{\pm}$) $\alpha_E = 2.0(6)(7) = -\beta_M$ (PDG)

$\alpha_E = 2.93(5),\ \beta_M = -2.77(11)$ (ChPT)

Neutral pion (π^0) $\alpha_E = -0.69(7)(4) = -\beta_M$ (PDG)

$\alpha_E = -0.40(18),\ \beta_M = 1.50(27)$ (ChPT)

Charged kaon ($K^{\pm}$) $\alpha_E = 0.58 = -\beta_M$ (ChPT)

IJMPA34 (2019) , Moinester and Scherer

Proton $\alpha_{E1} = 11.2(0.4),\quad \beta_{M1} = 2.5(1.2)$ (PDG)

$\alpha_{E1} = 11.2(0.7),\quad \beta_{M1} = 3.9(0.7)$ (ChPT)

$\gamma_{E1E1} = -3.3(0.8),\quad \gamma_{M1M1} = 2.9(1.5),$

$\gamma_{E1M2} = -0.2(0.2),\quad \gamma_{M1E2} = 1.1(0.3)$ (ChPT)

Neutron $\alpha_{E1} = 11.8(1.1),\quad \beta_{M1} = 3.7(1.2)$ (PDG)

$\alpha_{E1} = 13.7(3.1),\quad \beta_{M1} = 4.6(2.7)$ (ChPT)

$\gamma_{E1E1} = -4.7(1.1),\quad \gamma_{M1M1} = 2.9(1.5),$

$\gamma_{E1M2} = 0.2(0.2),\quad \gamma_{M1E2} = 1.6(0.4)$ (ChPT)

Eur. Phys. J. C75 (2015) Lensky, McGovern, Pascalutsa

Symmetry (2020), Hagelstein.

Background field vs. Four-point function

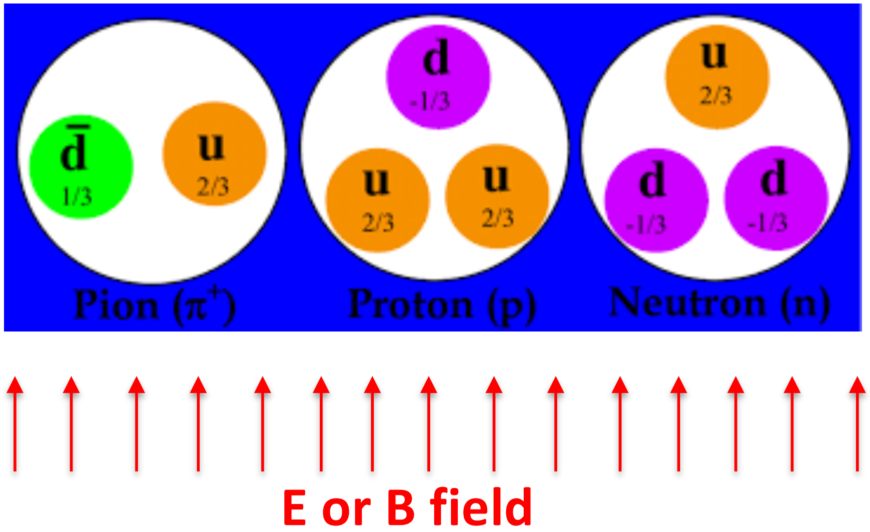

Energy shift under weak fields:

$$\Delta H = -\vec{\mu}\cdot\vec{B} - \frac{1}{2}\alpha E^2 - \frac{1}{2}\beta B^2 + \cdots$$

- Only two-point functions
- Works well for neutral hadrons (π^0, K^0, n)
- Challenges for charged particles: acceleration, Landau levels
- Active field of study

Recent review by G Endrodi, arXiv:2406.19780.

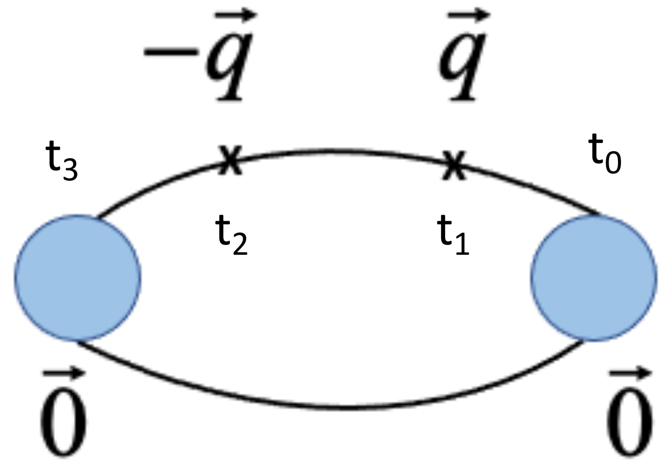

(zero momentum Breit frame)

- Mimics the Compton scattering process on the lattice
- Instead of background field, electromagnetic currents couple to quarks
- All photon, gluon, and quark interactions are included
- Charged hadron manifests as elastic form factors (charge radius).
- Renewed interest in lattice community

Formulas:
Charged pion vs Neutral pion

$$\alpha_E = \frac{\alpha \langle r_E^2 \rangle}{3m_\pi} + \frac{2\alpha}{\boldsymbol{q}^2} \int_0^\infty dt \left[Q_{44}(\boldsymbol{q}, t) - Q_{44}^{elas}(\boldsymbol{q}, t) \right]$$

$$\beta_M = -\frac{\alpha \langle r_E^2 \rangle}{3m_\pi} + \frac{2\alpha}{\boldsymbol{q}^2} \int_0^\infty dt \left[Q_{11}^{inel}(\boldsymbol{q}, t) - Q_{11}^{inel}(\boldsymbol{0}, t) \right]$$

Charge radius can be extracted from elastic part of the same Q_{44} ,

$$Q_{44}^{elas}(\boldsymbol{q}, t) = \frac{(E_\pi + m_\pi)^2}{4E_\pi m_\pi} F_\pi^2(\boldsymbol{q}^2)\, e^{-a(E_\pi(\boldsymbol{q}) - m_\pi)t}$$

4pt function also has access to form factors

Phys.Rev.D 108, 1, 014512 (2021)
Phys.Rev.D 108, 5, 054510 (2023)
Lee, Wilcox , Alexandru, Culver

$$\alpha_E = \lim_{\boldsymbol{q} \to 0} \frac{2\alpha}{\boldsymbol{q}^2} \int_0^\infty dt\, Q_{44}(\boldsymbol{q}, t)$$

$$\beta_M = \lim_{\boldsymbol{q} \to 0} \frac{2\alpha}{\boldsymbol{q}^2} \int_0^\infty dt \left[Q_{11}(\boldsymbol{q}, t) - Q_{11}(\boldsymbol{0}, t) \right]$$

- No elastic contributions for π^0
- Additional contributions from disconnected loops

Proton formulas

$$\alpha_E = \frac{\alpha\langle r_E^2\rangle}{3m_p} + \frac{\alpha(1+\kappa^2)}{4m_p^3} + \frac{2\alpha}{\boldsymbol{q}^2}\int_0^\infty dt\,\left[Q_{44}(\boldsymbol{q},t) - Q_{44}^{elas}(\boldsymbol{q},t)\right]$$

$$\beta_M = -\frac{\alpha\langle r_E^2\rangle}{3m_p} - \frac{\alpha(1+\kappa+\kappa^2)}{2m_p^3} + \frac{2\alpha}{\boldsymbol{q}^2}\int_0^\infty dt\,\left[Q_{11}(\boldsymbol{q},t) - Q_{11}^{elas}(\boldsymbol{q},t) - Q_{11}(\boldsymbol{0},t)\right]$$

$$Q_{44}^{elas}(\boldsymbol{q},t) \xrightarrow[t\gg 1]{} \left[1 - \boldsymbol{q}^2\left(\frac{1}{4m_p^2} + \frac{\langle r_E^2\rangle}{3}\right)\right] e^{-(E_p-m_p)t}$$

$$Q_{11}^{elas}(\boldsymbol{q},t) \xrightarrow[t\gg 1]{} \frac{(1+\kappa)^2}{4m_p^2}\boldsymbol{q}^2 e^{-(E_p-m_p)t}$$

PRD104 (2021), Wilcox, Lee

Neutron formulas

$$\alpha_E = \frac{\alpha\kappa^2}{4m_p^3} + \frac{2\alpha}{\boldsymbol{q}^2}\int_0^\infty dt\,Q_{44}(\boldsymbol{q},t)$$

$$\beta_M = -\frac{\alpha\kappa^2}{2m_p^3} + \frac{2\alpha}{\boldsymbol{q}^2}\int_0^\infty dt\,\left[Q_{11}(\boldsymbol{q},t) - Q_{11}^{elas}(\boldsymbol{q},t) - Q_{11}(\boldsymbol{0},t)\right]$$

$$Q_{11}^{elas}(\boldsymbol{q},t) \xrightarrow[t\gg 1]{} \frac{\kappa^2}{4m_p^2}\boldsymbol{q}^2 e^{-(E_p-m_p)t}$$

Operators

$$\frac{\sum_{\boldsymbol{x}_3,\boldsymbol{x}_2,\boldsymbol{x}_1,\boldsymbol{x}_0} e^{-i\boldsymbol{q}\cdot\boldsymbol{x}_2} e^{i\boldsymbol{q}\cdot\boldsymbol{x}_1} \langle\Omega|\psi^\dagger(x_3) : j^L_\mu(x_2) j^L_\nu(x_1) : \psi(x_0)|\Omega\rangle}{\sum_{\boldsymbol{x}_3,\boldsymbol{x}_0} \langle\Omega|\psi^\dagger(x_3)\psi(x_0)|\Omega\rangle}$$
$$\equiv Q_{\mu\nu}(\boldsymbol{q}, t_3, t_2, t_1, t_0)$$

Neutral pion: $\psi_{\pi^0}(x) = \frac{1}{\sqrt{2}}\left[\bar{u}(x)\gamma_5 u(x) - \bar{d}(x)\gamma_5 d(x)\right]$

Local current: $j^{(PC)}_\mu \equiv f\ Z_V \kappa\left(q_u \bar{u}\gamma_\mu u + q_d \bar{d}\gamma_\mu d\right)$

$$f = \{1, i\} \text{ for } \mu = \{4, 1\}$$

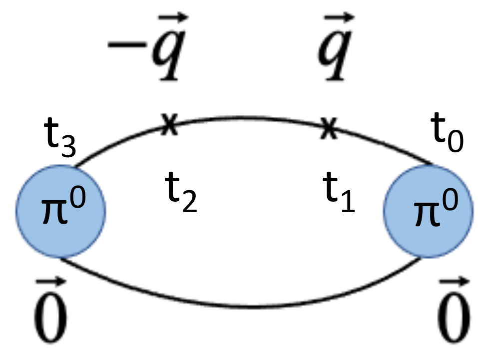

Conserved current (Z_V=1):

$$j^{(PS)}_\mu(x) \equiv f\, q_u \kappa_u\big[-\bar{u}(x)(1-\gamma_\mu)U_\mu(x)u(x+\hat{\mu}) + \bar{u}(x+\hat{\mu})(1+\gamma_\mu)$$
$$+ f\ q_d \kappa_d\big[-\bar{d}(x)(1-\gamma_\mu)U_\mu(x)d(x+\hat{\mu}) + \bar{d}(x+\hat{\mu})(1+\gamma_\mu)$$

Current conservation at momentum **q**=0 for Q_{44}:

$$\frac{\sum_{\boldsymbol{x}_3,\boldsymbol{x}_2,\boldsymbol{x}_1,\boldsymbol{x}_0} \langle\Omega|\psi(x_3) j^L_4(x_2) j^L_4(x_1)\psi^\dagger(x_0)|\Omega\rangle}{\sum_{\boldsymbol{x}_3,\boldsymbol{x}_0} \langle\Omega|\psi(x_3)\psi^\dagger(x_0)|\Omega\rangle} = q_1 q_2$$

(used for numerical validation of the diagrams)

Wick contractions

$$u\bar{u} - d\bar{d} \quad u\bar{u} + d\bar{d} \quad u\bar{u} + d\bar{d} \quad u\bar{u} - d\bar{d}$$

$$\begin{aligned}
g_4^{\mathrm{A}} &= 5\,\mathrm{tr}\left[S(t_1,t_3)\gamma_5 S(t_3,t_2)\gamma_\mu e^{-i\mathbf{q}} S(t_2,t_0)\gamma_5 S(t_0,t_1)\gamma_\mu e^{i\mathbf{q}}\right] \\
g_1^{\mathrm{A\text{-}bwd}} &= 5\,\mathrm{tr}\left[S(t_2,t_3)\gamma_5 S(t_3,t_1)\gamma_\mu e^{i\mathbf{q}} S(t_1,t_0)\gamma_5 S(t_0,t_2)\gamma_\mu e^{-i\mathbf{q}}\right] \\
g_{13}^{\mathrm{B}} &= 5\,\mathrm{tr}\left[S(t_2,t_3)\gamma_5 S(t_3,t_0)\gamma_5 S(t_0,t_1)\gamma_\mu e^{i\mathbf{q}} S(t_1,t_2)\gamma_\mu e^{-i\mathbf{q}}\right] \\
g_2^{\mathrm{B\text{-}bwd}} &= 5\,\mathrm{tr}\left[S(t_0,t_3)\gamma_5 S(t_3,t_2)\gamma_\mu e^{-i\mathbf{q}} S(t_2,t_1)\gamma_\mu e^{i\mathbf{q}} S(t_1,t_0)\gamma_5\right] \\
g_9^{\mathrm{C}} &= 5\,\mathrm{tr}\left[S(t_1,t_3)\gamma_5 S(t_3,t_0)\gamma_5 S(t_0,t_2)\gamma_\mu e^{-i\mathbf{q}} S(t_2,t_1)\gamma_\mu e^{i\mathbf{q}}\right] \\
g_7^{\mathrm{C\text{-}bwd}} &= 5\,\mathrm{tr}\left[S(t_0,t_3)\gamma_5 S(t_3,t_1)\gamma_\mu e^{i\mathbf{q}} S(t_1,t_2)\gamma_\mu e^{-i\mathbf{q}} S(t_2,t_0)\gamma_5\right] \\
g_8^{\mathrm{D}} &= -10\,\mathrm{tr}\left[S(t_0,t_3)\gamma_5 S(t_3,t_0)\gamma_5\right]\mathrm{tr}\left[S(t_1,t_2)\gamma_\mu e^{-i\mathbf{q}} S(t_2,t_1)\gamma_\mu e^{i\mathbf{q}}\right] \\
g_{12}^{\mathrm{El}} &= -1\,\mathrm{tr}\left[S(t_1,t_3)\gamma_5 S(t_3,t_0)\gamma_5 S(t_0,t_1)\gamma_\mu e^{i\mathbf{q}}\right]\mathrm{tr}\left[S(t_2,t_2)\gamma_\mu e^{-i\mathbf{q}}\right] \\
g_0^{\mathrm{El\text{-}bwd}} &= -1\,\mathrm{tr}\left[S(t_0,t_3)\gamma_5 S(t_3,t_1)\gamma_\mu e^{i\mathbf{q}} S(t_1,t_0)\gamma_5\right]\mathrm{tr}\left[S(t_2,t_2)\gamma_\mu e^{-i\mathbf{q}}\right] \\
g_{10}^{\mathrm{Er}} &= -1\,\mathrm{tr}\left[S(t_2,t_3)\gamma_5 S(t_3,t_0)\gamma_5 S(t_0,t_2)\gamma_\mu e^{-i\mathbf{q}}\right]\mathrm{tr}\left[S(t_1,t_1)\gamma_\mu e^{i\mathbf{q}}\right] \\
g_5^{\mathrm{Er\text{-}bwd}} &= -1\,\mathrm{tr}\left[S(t_0,t_3)\gamma_5 S(t_3,t_2)\gamma_\mu e^{-i\mathbf{q}} S(t_2,t_0)\gamma_5\right]\mathrm{tr}\left[S(t_1,t_1)\gamma_\mu e^{i\mathbf{q}}\right] \\
g_{11}^{\mathrm{F}} &= 2\,\mathrm{tr}\left[S(t_0,t_3)\gamma_5 S(t_3,t_0)\gamma_5\right]\mathrm{tr}\left[S(t_2,t_2)\gamma_\mu e^{-i\mathbf{q}}\right]\mathrm{tr}\left[S(t_1,t_1)\gamma_\mu e^{i\mathbf{q}}\right] \\
g_3^{\mathrm{G}} &= -9\,\mathrm{tr}\left[S(t_2,t_3)\gamma_5 S(t_3,t_2)\gamma_\mu e^{-i\mathbf{q}}\right]\mathrm{tr}\left[S(t_0,t_1)\gamma_\mu e^{i\mathbf{q}} S(t_1,t_0)\gamma_5\right] \\
g_6^{\mathrm{H}} &= -9\,\mathrm{tr}\left[S(t_1,t_3)\gamma_5 S(t_3,t_1)\gamma_\mu e^{i\mathbf{q}}\right]\mathrm{tr}\left[S(t_0,t_2)\gamma_\mu e^{-i\mathbf{q}} S(t_2,t_0)\gamma_5\right].
\end{aligned}$$

Quark propagator $S_q(t_2,t_1) \equiv \langle q\bar{q}\rangle = \dfrac{1}{\not{D} + m_q}$

Connected contributions

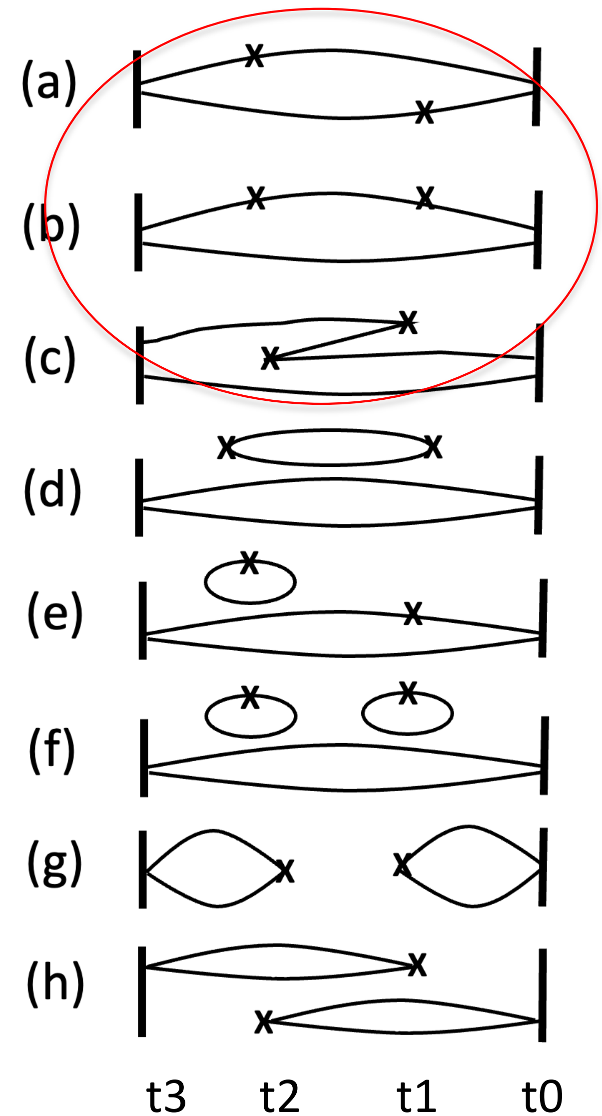

Simulation details

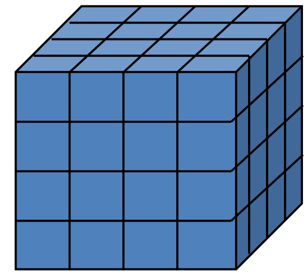

Proof-of-concept simulation:

- Quenched Wilson action on 24^3x48 lattice with spacing a=0.085 fm.
- Dirichlet boundary condition in time, periodic in space.
- Quark mass parameter κ=0.1520, 0.1543, 0.1555, 0.1565 corresponding to pion mass m_π=1100, 800, 600, 370 MeV. Analyzed 1000 configurations for each mass.
- 5 momenta **q**={0,0,0}, {0,0,1}, {0,1,1}, {1,1,1}, {0,0,2} per mass

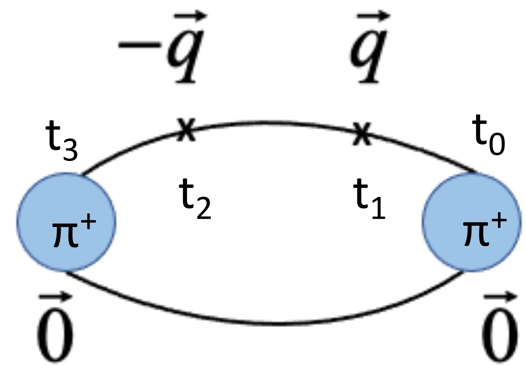

Dynamical ensembles in progress:

nhyp 2-flavor clover fermion
+ Lüscher-Weiz gauge action

Label	$N_t \times N_{x,y}^2 \times N_z$	η	a[fm]	N_{cfg}	am_π
$\mathcal{E}_1$	$48 \times 24^2 \times 24$	1.00	0.1210(2)(24)	300	0.1931(4)
$\mathcal{E}_2$	$48 \times 24^2 \times 30$	1.25	–	–	0.1944(3)
$\mathcal{E}_3$	$48 \times 24^2 \times 48$	2.00	–	–	0.1932(3)
$\mathcal{E}_4$	$64 \times 24^2 \times 24$	1.00	0.1215(3)(24)	400	0.1378(6)
$\mathcal{E}_5$	$64 \times 24^2 \times 28$	1.17	–	–	0.1374(5)
$\mathcal{E}_6$	$64 \times 24^2 \times 32$	1.33	–	–	0.1380(5)

TABLE I. Details of the $N_f = 2$ ensembles used in this study. Here η is elongation in the z-direction, a the lattice spacing, N_{cfg} the number of Monte Carlo configurations. Ensembles $\mathcal{E}_1, \mathcal{E}_2, \mathcal{E}_3$ have a pion mass $m_\pi \approx 315$ MeV, while $\mathcal{E}_4, \mathcal{E}_5, \mathcal{E}_6$ have a pion mass $m_\pi \approx 220$ MeV.

Four-point functions Q_{44} for α_E

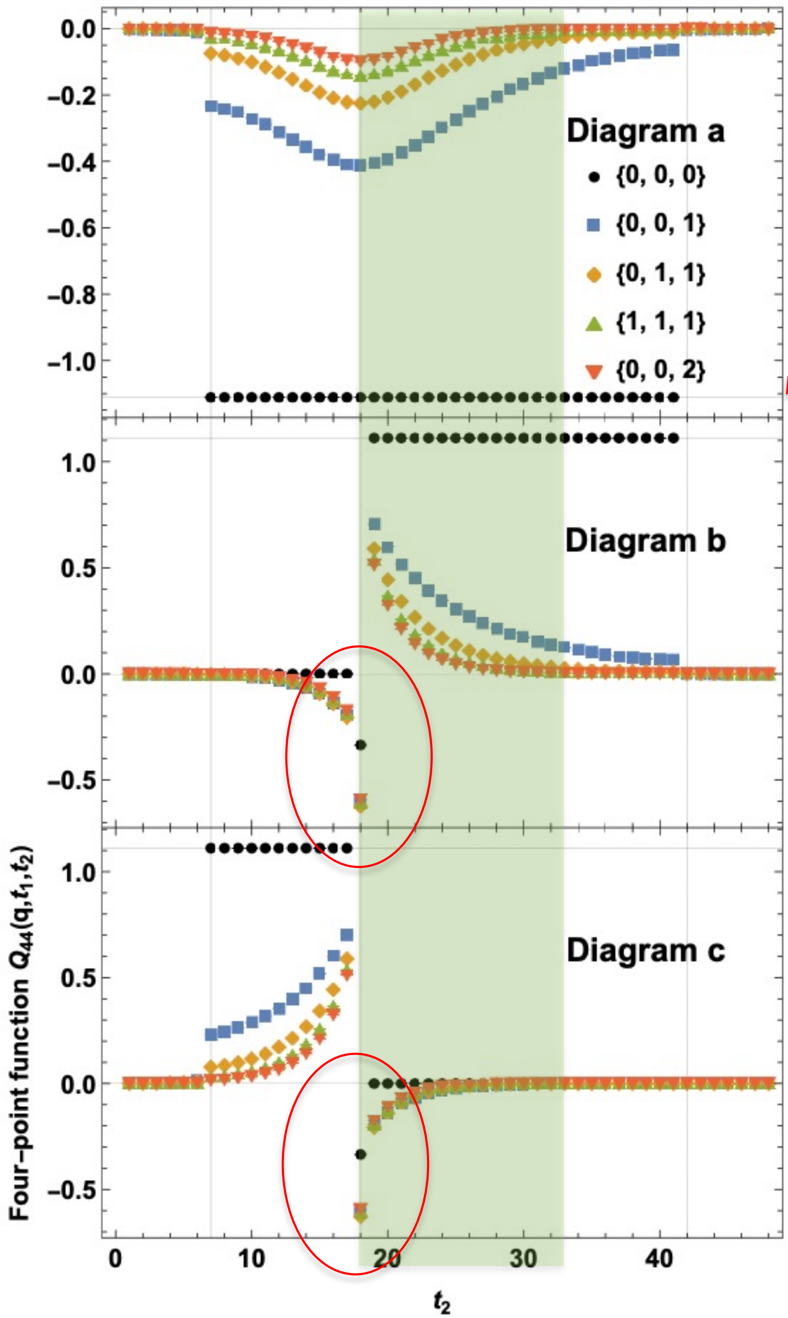

$$-10/9 = 2(q_u q_{\bar{u}} + q_d q_{\bar{d}})$$

(current conservation at **q**=0)

$$10/9 = 2(q_u q_u + q_d q_d) = 2(q_{\bar{u}} q_{\bar{u}} + q_{\bar{d}} q_{\bar{d}})$$

(current conservation at **q**=0)

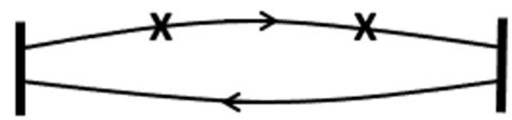

$$10/9 = 2(q_u q_u + q_d q_d) = 2(q_{\bar{u}} q_{\bar{u}} + q_{\bar{d}} q_{\bar{d}})$$

(current conservation at **q**=0)

Diagram b and c have unphysical contact interactions (we avoid $t_1=t_2$)

Four-point functions Q_{11} for β_M

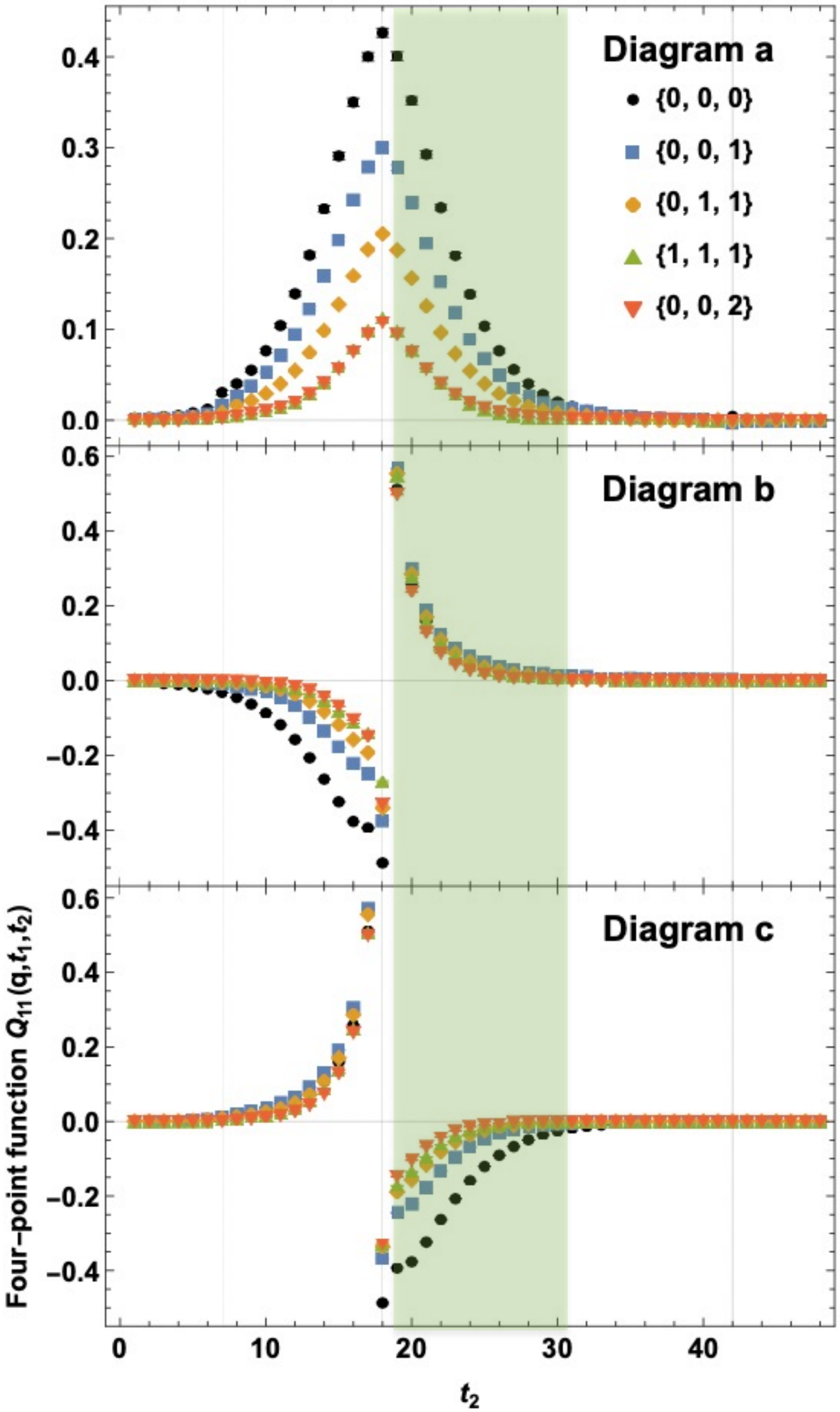

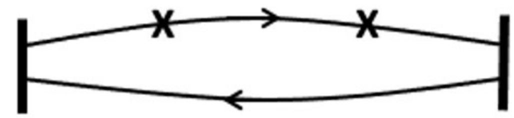

Time integrals

$$\alpha_E = \lim_{\boldsymbol{q}\to 0} \frac{2\alpha}{\boldsymbol{q}^2} \int_0^\infty dt\, Q_{44}(\boldsymbol{q}, t)$$

$$\beta_M = \lim_{\boldsymbol{q}\to 0} \frac{2\alpha}{\boldsymbol{q}^2} \int_0^\infty dt \left[Q_{11}(\boldsymbol{q}, t) - Q_{11}(\boldsymbol{0}, t) \right]$$

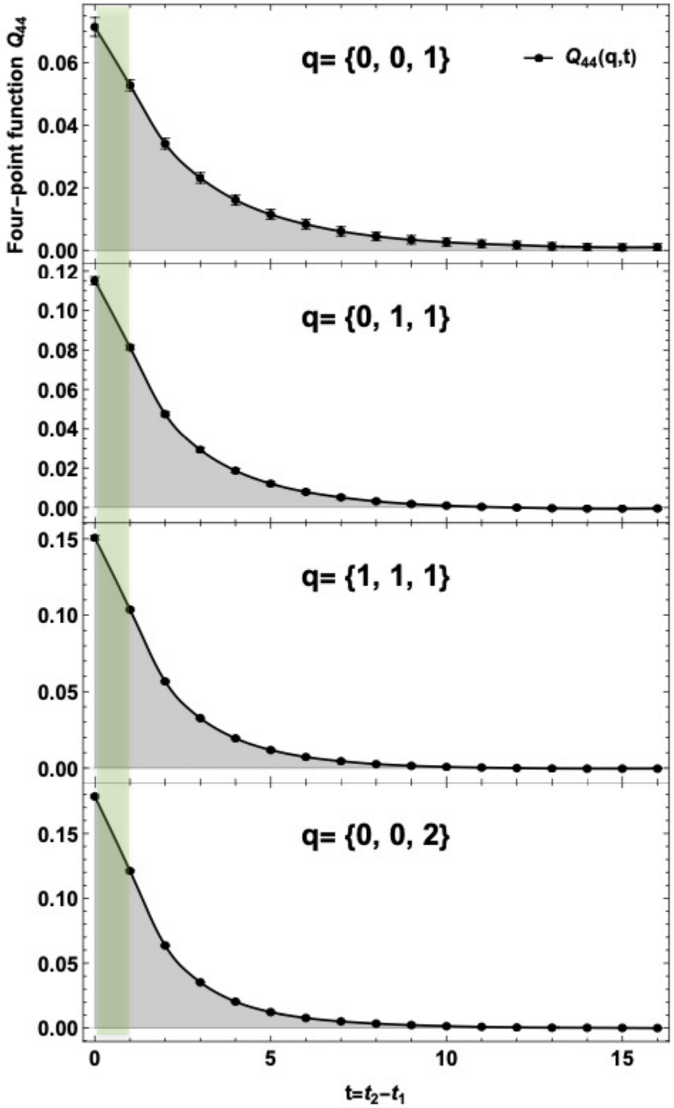

Signal is shaded area

Extrapolation from t=1 to t=0

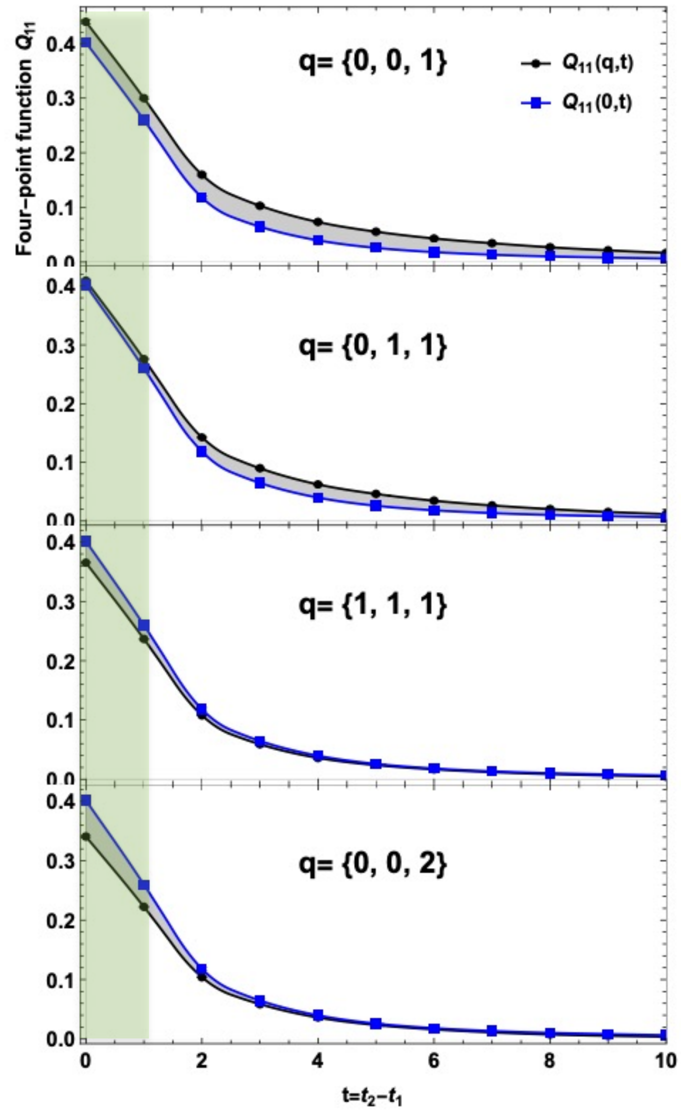

Signal changes sign

Extrapolation to $\mathbf{q}^2$=0

$$\alpha_E = \lim_{\boldsymbol{q}\to 0} \frac{2\alpha}{\boldsymbol{q}^2} \int_0^\infty dt\, Q_{44}(\boldsymbol{q},t)$$

$$\beta_M = \lim_{\boldsymbol{q}\to 0} \frac{2\alpha}{\boldsymbol{q}^2} \int_0^\infty dt \Big[Q_{11}(\boldsymbol{q},t) - Q_{11}(\boldsymbol{0},t) \Big]$$

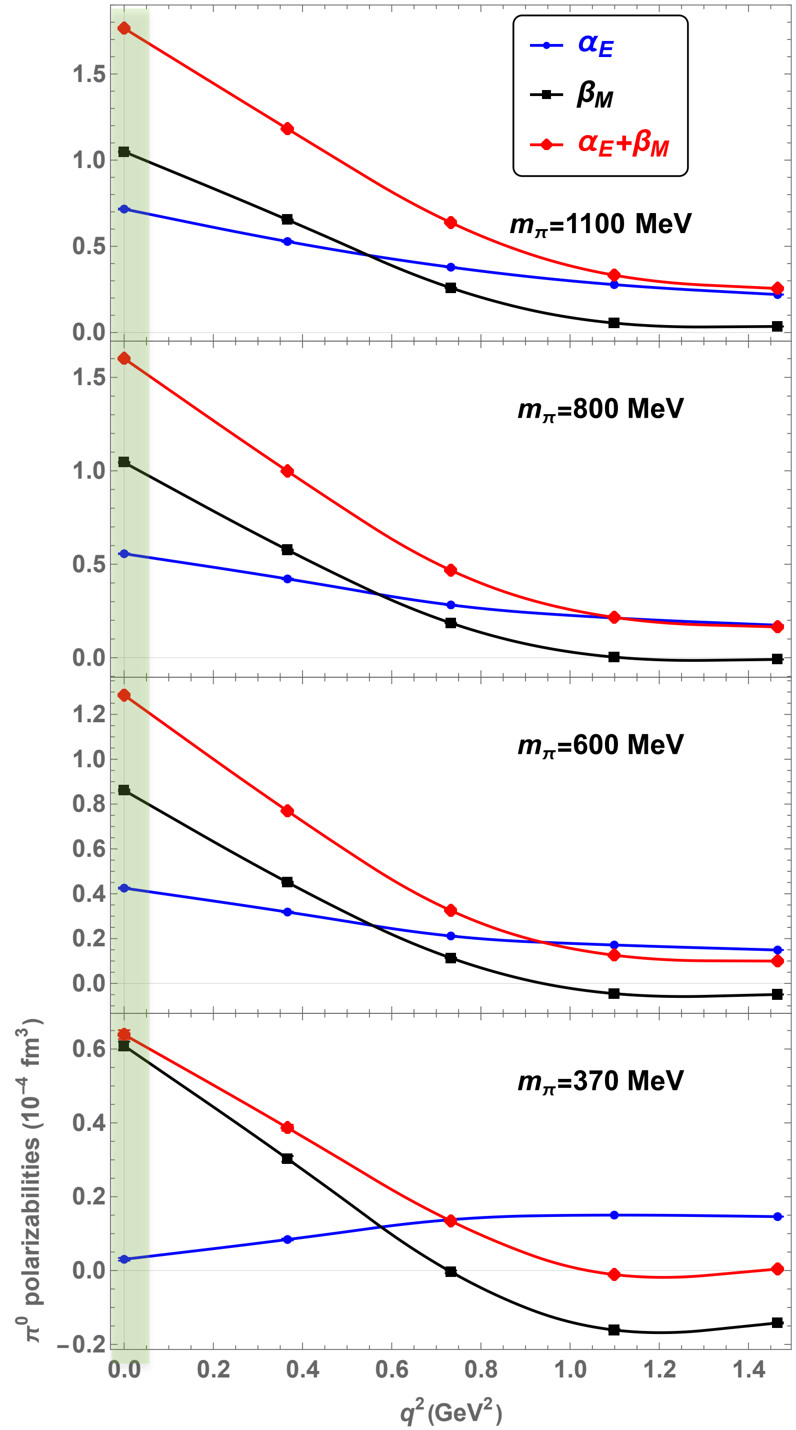

Chiral extrapolation

$$\alpha_E = \lim_{\boldsymbol{q}\to 0} \frac{2\alpha}{\boldsymbol{q}^2} \int_0^\infty dt\, Q_{44}(\boldsymbol{q}, t) \qquad \beta_M = \lim_{\boldsymbol{q}\to 0} \frac{2\alpha}{\boldsymbol{q}^2} \int_0^\infty dt \Big[Q_{11}(\boldsymbol{q}, t) - Q_{11}(\boldsymbol{0}, t) \Big]$$

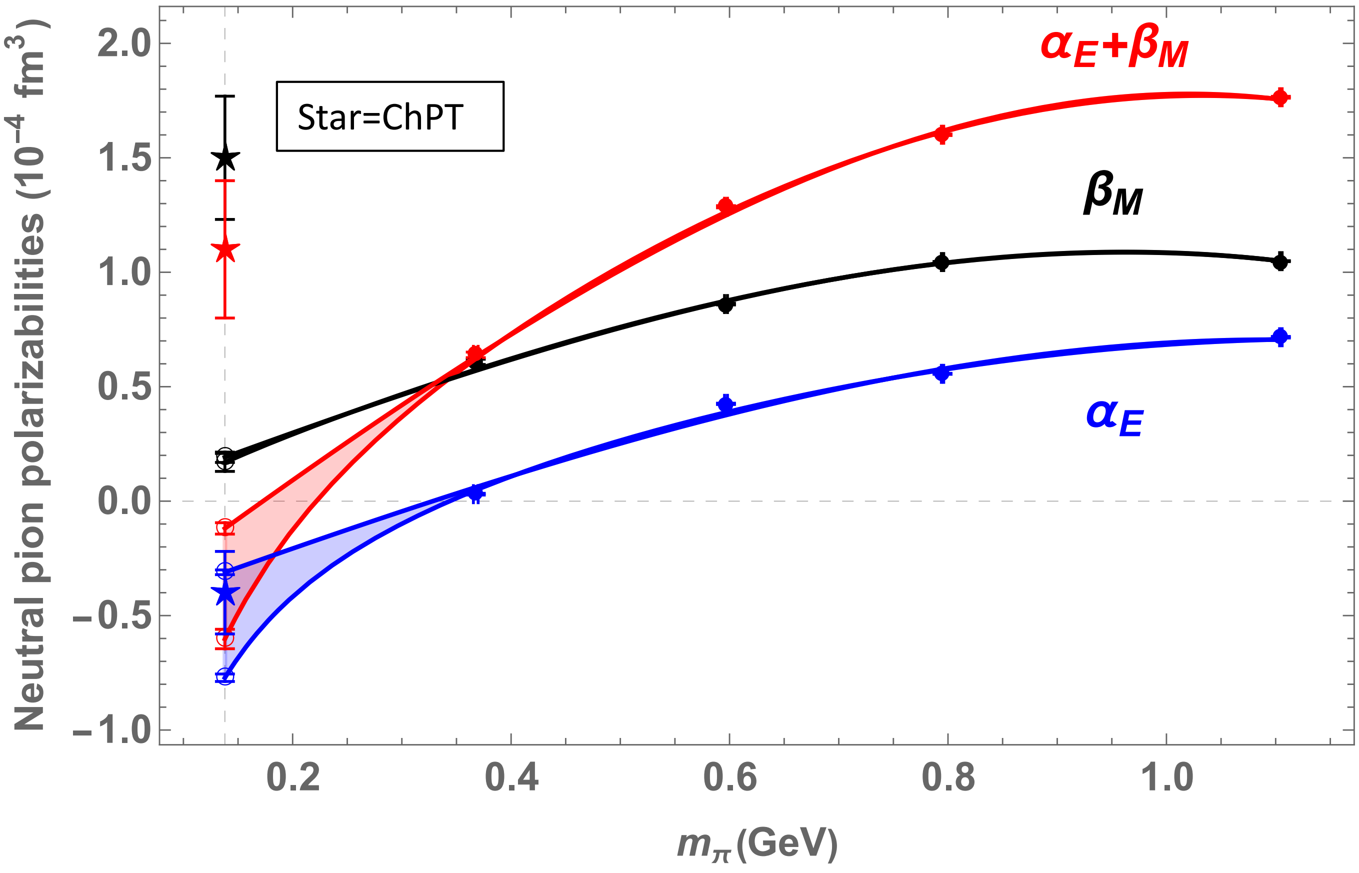

$$a + b\, m_\pi + c\, m_\pi^3$$

$$\frac{a}{m_\pi} + b\, m_\pi + c\, m_\pi^3$$

Electric is consistent with ChPT.
Magnetic has large discrepancy.

Neutral pion vs Charged pion

$$\alpha_E = \lim_{\boldsymbol{q}\to 0} \frac{2\alpha}{\boldsymbol{q}^2} \int_0^\infty dt\, Q_{44}(\boldsymbol{q}, t)$$

$$\beta_M = \lim_{\boldsymbol{q}\to 0} \frac{2\alpha}{\boldsymbol{q}^2} \int_0^\infty dt \left[Q_{11}(\boldsymbol{q}, t) - Q_{11}(\boldsymbol{0}, t) \right]$$

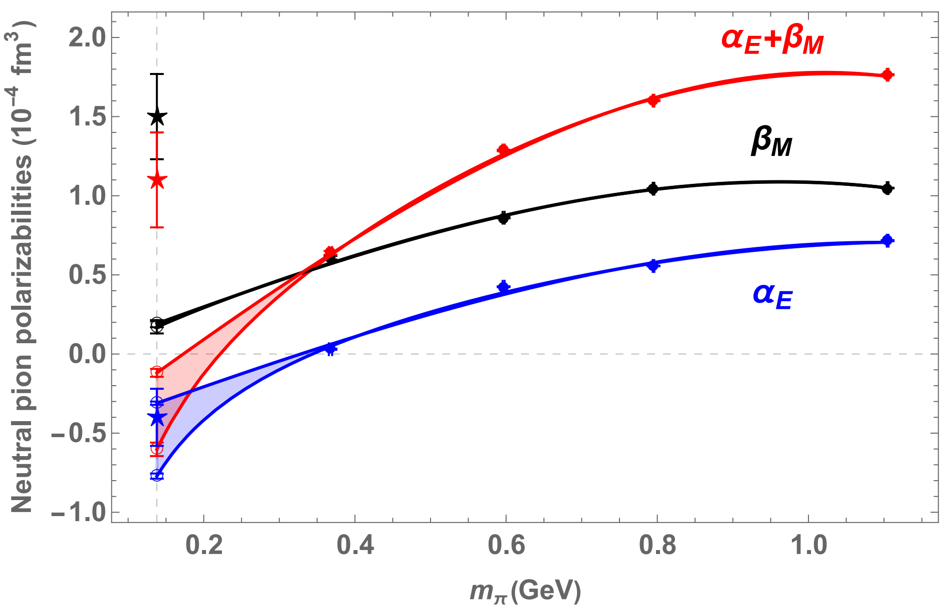

Electric is consistent with ChPT.
Magnetic has large discrepancy.

$$\alpha_E = \frac{\alpha \langle r_E^2 \rangle}{3m_\pi} + \frac{2\alpha}{\boldsymbol{q}^2} \int_0^\infty dt \left[Q_{44}(\boldsymbol{q}, t) - Q_{44}^{elas}(\boldsymbol{q}, t) \right]$$

$$\beta_M = -\frac{\alpha \langle r_E^2 \rangle}{3m_\pi} + \frac{2\alpha}{\boldsymbol{q}^2} \int_0^\infty dt \left[Q_{11}^{inel}(\boldsymbol{q}, t) - Q_{11}^{inel}(\boldsymbol{0}, t) \right]$$

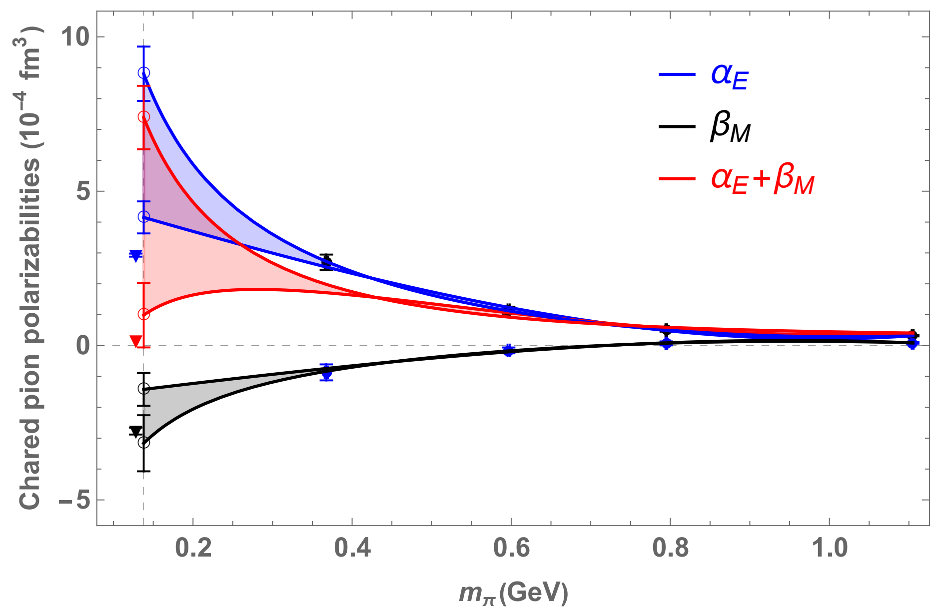

Electric is larger than ChPT.
Magnetic is consistent with ChPT.

Four-point function vs. Background field

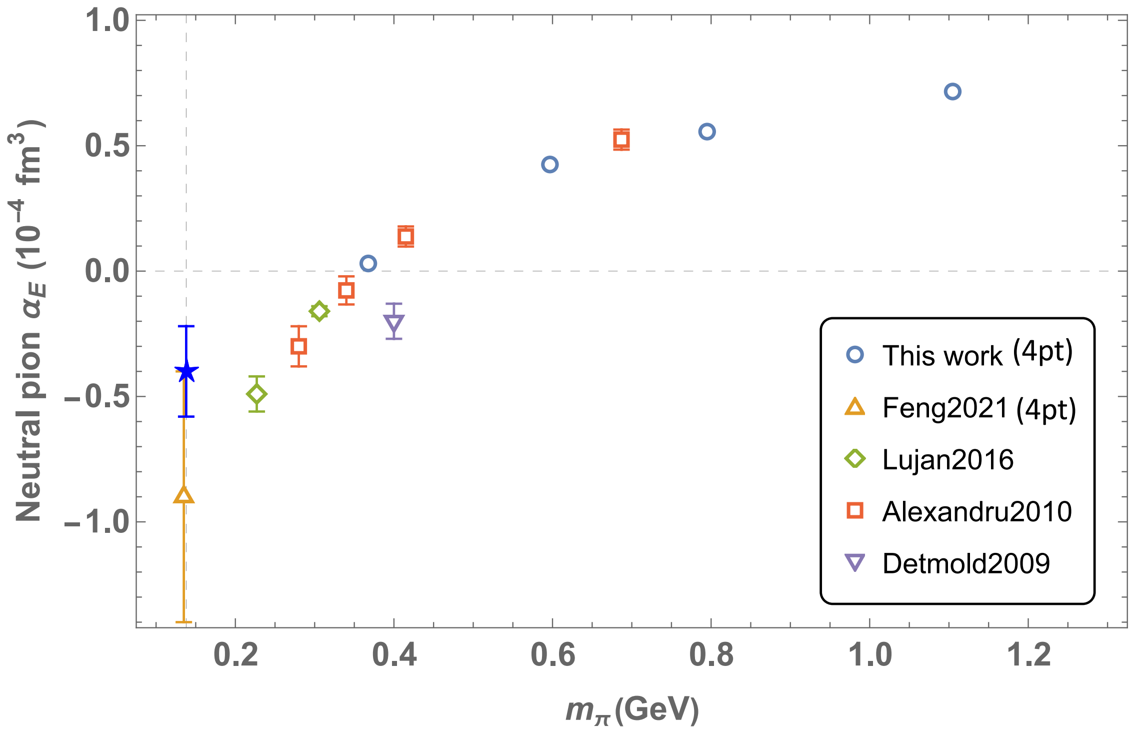

Electric: largely consistent

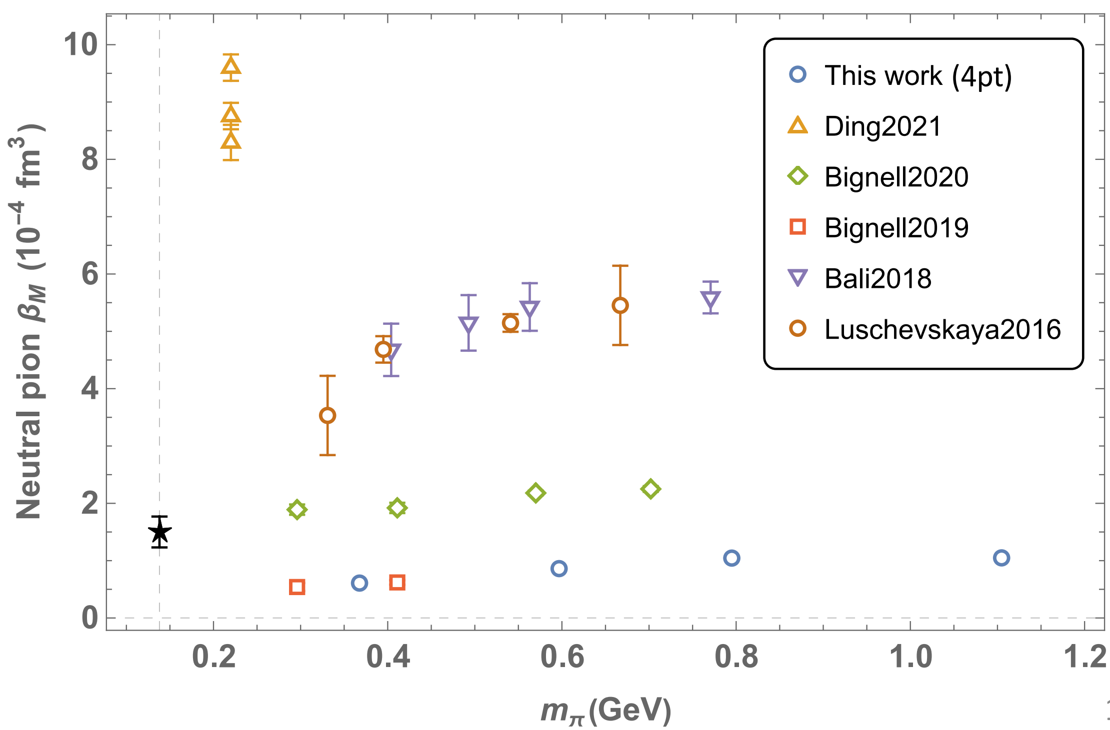

Magnetic: large disagreements

Conclusion

- Four-point functions offer a clear picture of how polarizabilities arise in QCD+QED.
  - π^0 has no charge radius contribution, but additional disconnected terms, compared to π^+
  - Only need 2pt and 4pt (but not 3pt) functions

- Open issues
  - Extrapolation to t=0 (contact term)
  - Quenched approximation
  - Only connected contributions so far
  - Large discrepancy with background field method for π^0 magnetic polarizability (β_M)

- Outlook
  - Dynamical ensembles under way (two-flavor nHYP-clover, 315 and 227 MeV, elongated geometries for volume study and smaller $\mathbf{q}^2$)
  - Include disconnected contributions